Precise Control of Ferrite Phase Shifters*

D. D. KING†, C. M. BARRACK‡, AND C. M. JOHNSON†

Summary—**Hysteresis and thermal drifts can prevent accurate calibration of ferrite phase shifters. To provide a precise setting of phase in response to a control signal a servo system has been developed. This system utilizes a control frequency to determine uniquely the phase shift in a ferrite element. The desired phase shift is then a function only of control frequency and line length. Performance data are given for various operating conditions of the control system.**

Introduction

ELECTRICAL control of the phase shift in transmission line and waveguide elements has many applications, notably in antenna arrays. Ferrite phase shifters giving phase changes of 360 degrees or more with very low loss have been developed, particularly at the higher microwave frequencies.[1] Perhaps the principal drawback of these devices is their poor calibration accuracy. Hysteresis can cause changes of 30 degrees or more in the phase shift prevailing at a given applied magnetic field. In some cases, thermal drifts may also alter the phase shift obtained. The circuits described in this paper permit a precise electrical control of phase shift that is independent of any hysteresis or thermal drifts in the ferrite. A somewhat similar scheme has been described for phase measurement.[2]

Frequency Controlled Phase Shifter

The frequency controlled phase shifter consists of an electrically variable phase shifting element, a comparison loop, and a feedback control system. In the simplest version of this device, the insertion phase shift is controlled precisely by the frequency of a control signal sent through the same line as the signal whose phase is to be varied. A schematic diagram of the device is shown in Fig. 1.

The phase changing element shown with a control coil may be any electrically variable phase shifter in any type of transmission line or guide. Both reciprocal and nonreciprocal devices can be controlled in the same manner. The control current or voltage is furnished through a servo amplifier coupled to a phase detector in the comparison loop. The position of the phase detector is indicated by a dotted reference plane in Fig. 1.

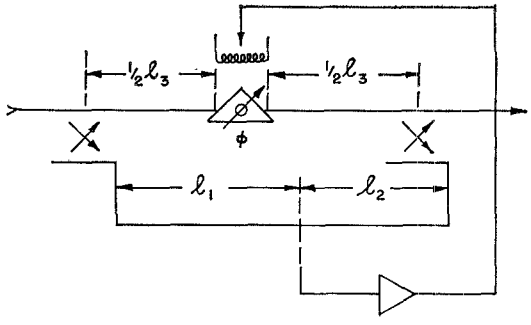

Fig. 1—Frequency controlled phase shifter.

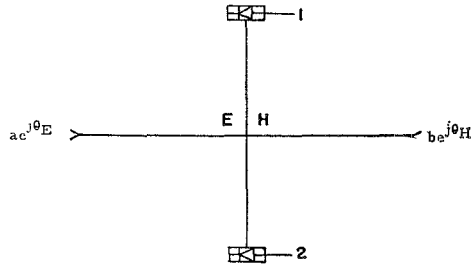

Fig. 2—Hybrid sensing element.

A pair of probes or a balanced loop are possible phase detectors, but a hybrid junction seems best suited for the needs of this circuit.

A hybrid sensing element placed at the reference plane in Fig. 1 receives signals from both directional couplers. These waves enter the shunt and series arms, as shown in Fig. 2. Balanced crystals are mounted in the side arms, so the entire unit is identical with a standard balanced mixer assembly.

In terms of the two input waves, the voltage amplitudes at the two crystals are

$$A_1 = (1/\sqrt{2})ae^{j\theta}E + (1/\sqrt{2})\,be^{j\theta_H} = \left[1 + \frac{b}{a}\,e^{j(\theta_H-\theta_E)}\right]\left[\frac{a}{\sqrt{2}}\,e^{j\theta_E}\right] \tag{1a}$$

$$A_2 = -(1/\sqrt{2})ae^{j\theta_E} + (1/\sqrt{2})\,be^{\theta_{jH}} = \left[1 - \frac{b}{a}\,e^{j(\theta_H-\theta_E)}\right]\left[\frac{a}{\sqrt{2}}\,e^{\theta_{jE}}\right]. \tag{1b}$$

The signal difference of the two crystals is

$$|A_1| - |A_2| = \frac{a}{\sqrt{2}}\left\{\left|1 + \frac{b}{a}\,e^{j\Delta\theta}\right| - \left|1 - \frac{b}{a}\,e^{j\Delta\theta}\right|\right\} \tag{2}$$

where $\Delta\theta = \theta_H - \theta_E$.

* Original manuscript received by the PGMTT, July 16, 1958; revised manuscript received, September 25, 1959.
This work was sponsored by ARDC's Rome Air Dev. Center under Contract AF 30(602)-1776.
† Electronic Communications, Inc., Timonium, Md.
‡ Miller Research Laboratories, Baltimore, Md., formerly Electronic Communications, Inc., Timonium, Md.
[1] F. Reggia and E. G. Spencer, "A new technique in ferrite phase shifting for beam scanning of microwave antennas," PROC. IRE, vol. 45, pp. 1510–1517; November, 1957.
[2] H. A. Dropkin, "Direct reading microwave phase meter," IRE CONVENTION RECORD, pt. 1, pp. 57–63; March, 1958.

When $\Delta\theta=\pi/2$, the difference output is zero, corresponding to a bridge balance. For smaller values of $\Delta\theta$, the difference is positive; for larger values it is negative. Adequate sense information is, therefore, provided for maintaining a balance condition at $\Delta\theta=\pi/2$. With a servo amplifier it is then possible to position the standing wave pattern by controlling the phase θ_H of the output wave. The position of the standing wave pattern is also a function of relative line lengths and of the frequency. The relationship between these quantities is now examined quantitatively.

From Fig. 1, the condition for balance (zero difference output) at the hybrid junction can be written down in terms of individual phase delays. It is

$$\phi+\frac{2\pi}{\lambda}(l_3+l_2)=\frac{2\pi}{\lambda}l_1\pm(2n+1)\frac{\pi}{2}. \tag{3}$$

Eq. (3) is multiple valued with interval π. However, the slope of the error signal versus angular deviation curve given by (2) alternates in sign from one balance point to another. Once negative feedback has been established for a particular control amplifier, the system is then stable only at alternate balance points having the proper slope. Therefore, the effective balance equation is periodic with an interval 2π.

$$\phi=\frac{2\pi}{\lambda}(l_3+l_2)=\frac{2\pi}{\lambda}l_1\pm(4n+1)\frac{\pi}{2}. \tag{4}$$

A path difference l may be defined:

$$l=l_1-(l_2+l_3). \tag{5}$$

The normalized phase shift introduced by the phase shifter being controlled then becomes

$$\frac{\phi}{2\pi}=\frac{l}{\lambda}\pm\frac{4n+1}{4}. \tag{6}$$

The phase excursion is assumed to run from $\phi_1=0$ to $\phi_2=m\pi$ radians. The balance (6) then becomes

$$\frac{l}{\lambda_1}=\frac{4n_1+1}{4}\qquad(\phi_1=0) \tag{7}$$

$$\frac{l}{\lambda_2}=\frac{4n_2+2m+1}{4}\qquad(\phi_2=m\pi). \tag{8}$$

The difference in wave numbers between the two expressions is

$$\frac{1}{\lambda_1}-\frac{1}{\lambda_2}=\frac{1}{l}\left(n_1-n_2-\frac{m}{2}\right). \tag{9}$$

For $m\leq 2$, corresponding to the gamut of useful excursions, $0<\phi<2\pi$, the difference in wave numbers can be kept to one or less. This eliminates the possibility of ambiguities from $n_1\neq n_2$, *i.e.*, from harmonic operation.

The minimum path difference l for a 360 degree phase shift occurs for $n=0$. Then (7) and (8) yield,

$$l=\frac{\lambda_1}{4}=\frac{5\lambda_2}{4};\qquad\frac{\lambda_1}{\lambda_2}=5.$$

To achieve a small ratio of wavelengths, higher values of n may be chosen. For example, for $n=5$,

$$l=\frac{21}{4}\lambda_1=\frac{25}{4}\lambda_2:\frac{\lambda_1}{\lambda_2}=\frac{25}{21}.$$

By suitable choice of the path difference l, all control frequencies f_c necessary to produce phase shifts in the interval $0<\phi<2\pi$ can be located in a narrow interval $f_1\leq f_c\leq f_2$. This interval is chosen to lie close to the signal frequency f. The phase shift at the signal frequency then differs by a negligible amount from its precisely determined value at the control frequency. A discussion of servo operation and limits of error is deferred to a later section.

A typical system for precise electronic phase control is shown in Fig. 3.

Only milliwatts are required to operate the servo; hence, the control signal need not be large. In waveguide systems, a beyond-cut-off section in the directional coupler suffices to eliminate coupling to a lower signal frequency.

Heterodyne Controlled Phase Shifter

The circuit of Fig. 3 may be modified in a simple but significant way by inserting two mixers in place of the filters. The revised system appears in Fig. 4.

Since the mixing operation is linear, phases are preserved. With equiphase injection of the control or local oscillator signal, the relative phases of the signals in the lower part of the control loop remain the same, but are referred to the sum or difference frequency $f'=f\pm f_c$. For sum frequency operation (5) need only be scaled to the different wavelengths in the upper and lower portions of the control loop.

$$\frac{l}{\lambda'}=\frac{l_1}{\lambda'}-\left(\frac{l_2}{\lambda'}+\frac{l_3}{\lambda}\right)$$

or

$$l=l_1-l_2-l_3\left(\frac{\lambda'}{\lambda}\right). \tag{10}$$

The average wavelength in the loop is now shorter; hence, a more compact structure is possible. Operation at the difference frequency with low-frequency discriminators is also feasible.

The actual signal phase shift is controlled in the heterodyne system, rather than the phase shift at a nearby frequency. This eliminates the need for filters, and provides absolute accuracy. However, the modulation characteristic of the signal must permit the servo to operate. In general, very short duty cycles and rapid frequency modulations are not suitable for this purpose.

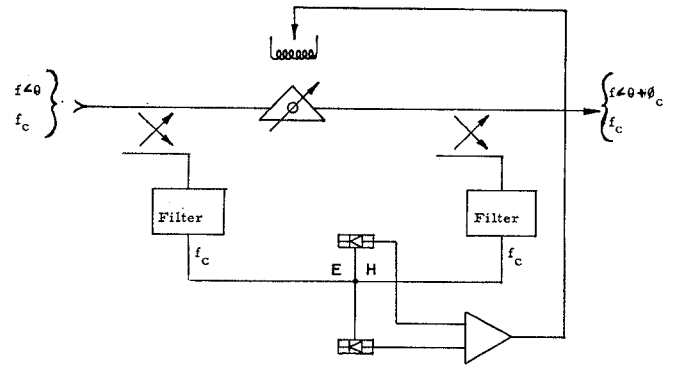

Fig. 3—Phase control system.

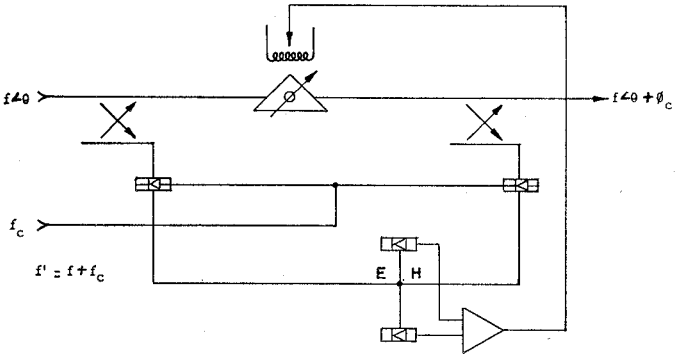

Fig. 4—Heterodyne phase control system.

The previously described system using separate control frequencies is, of course, free from such limitations.

Proportional Control Servo

The servo system applies a control voltage to the active element controlling the current through the ferrite phase shifter coil. This control voltage is generated in response to an error signal developed at the hybrid junction. The functional relationship between error signal magnitude and phase error can be derived directly in terms of the quantities in Fig. 2.

Eq. (2) is the starting point for the calculation, and is written explicitly below.

$$|A_1| - |A_2| = \frac{a}{\sqrt{2}}\left\{\left(\frac{b}{a}\cos\Delta\theta + 1\right)^2 + \left(\frac{b}{a}\sin\Delta\theta\right)^2\right\}^{1/2} - \frac{a}{\sqrt{2}}\left\{\left(\frac{b}{a}\cos\Delta\theta - 1\right)^2 + \left(\frac{b}{a}\sin\Delta\theta\right)^2\right\}^{1/2}. \quad (11)$$

The difference vanishes for $\Delta\theta = (2n+1)\,\pi/2$, as noted in connection with (3) previously. To represent this explicitly, we write

$$\Delta\theta = (2n+1)\frac{\pi}{2} + \epsilon \quad (12)$$

where ϵ is the phase deviation from the balance condition. Inserting (12) into (11) and assuming an identical detection efficiency β for each crystal yields the following exact relation between difference output Δe and the phase error ϵ.

$$\frac{\Delta e}{a} = \frac{\beta}{\sqrt{2}}\left\{\left(\frac{b}{a}\right)^2 + 1 - \frac{2b}{a}(-1)^n\sin\epsilon\right\}^{1/2} - \frac{\beta}{\sqrt{2}}\left\{\left(\frac{b}{a}\right)^2 + 1 + \frac{2b}{a}(-1)^n\sin\epsilon\right\}^{1/2}. \quad (13)$$

For operation near the balance point, only small errors apply, and (13) can be expanded,

$$\frac{\Delta e}{a} = -\beta\epsilon\left\{\frac{\sqrt{2}(-1)^n}{(1+(a/b)^2)^{1/2}}\right\}. \quad (14)$$

The ratio of input amplitudes evidently has only a second order effect on the sensitivity. By keeping $b>a$, the maximum phase sensitivity is achieved. Per unit amplitude in the E arm (14) can then be written as

$$\Delta e \sim -\beta\epsilon\sqrt{2}(-1)^n. \quad (15)$$

The factor $(-1)^n$ shows that the control loop feedback is either positive or negative, depending on the interval of π occupied by the phase shift. Choosing the sign of feedback therefore determines whether n is even or odd for stable balance. This effectively makes the system periodic in 2π, as indicated previously.

For unit rectification efficiency, (15) yields a sensitivity

$$\Delta e \approx 25 \text{ millivolts/degree phase error.} \quad (16)$$

Experimental Results

To demonstrate the operation of the frequency control system under both open and closed loop conditions, a phase comparison bridge was assembled for C-band operation. The measurement system utilizes two reflex klystrons, one, furnishing the control frequency for the phase shifter and the other, simulating the signal frequency whose phase is to be controlled. In this test system beyond-cut-off waveguide for the signal frequency is not used for the control loop. Instead, the control frequency is propagated in the opposite direction from the signal frequency, and directional couplers are oriented to accept only the control frequency into the loop. This arrangement assumes a reciprocal phase shifter.

A simple dc control amplifier with a voltage gain of about 62 db is used in the servo loop. The phase shifter in the control loop uses Trans-Tech type TT-414 ferrite. This material was used because of its availability and is probably not optimum for C-band use. The ferrite element is a strip .2″×.4″×6.0″ mounted vertically in the center of a section of standard 1″×.5″ waveguide filled with teflon. A longitudinal external magnetic field produces the phase shift in the ferrite. Two series of tests were made on the complete phase shifter control loop. In the first measurements the ferrite phase shifter solenoid was disconnected. The control frequency was then

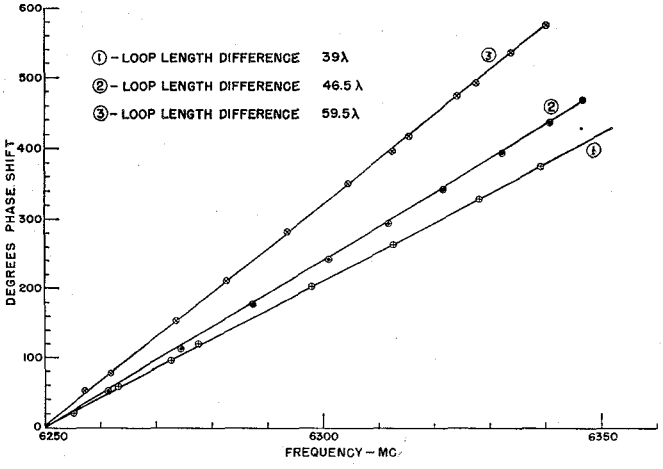

Fig. 5—Loop characteristics, manual control.

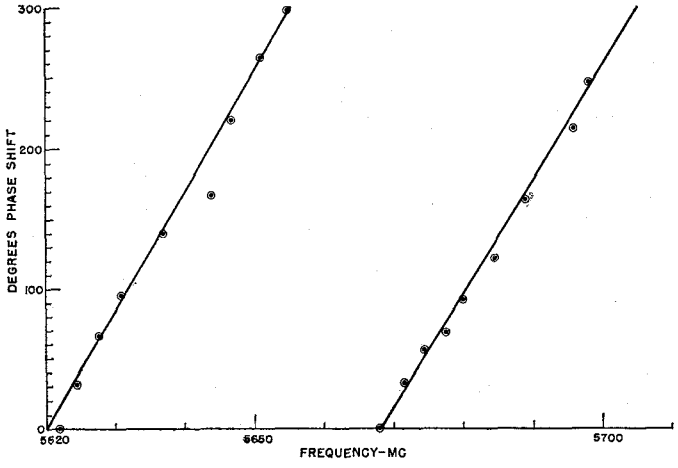

Fig. 6—Loop characteristics, servo control.

changed and the loop was balanced manually by varying a precision phase shifter in one of the loop arms. This measurement was repeated for several different lengths of one branch of the control loop. In the second group of tests the servo system was active. The control frequency was varied and the resulting change in phase of the operating signal was measured. This measurement was also repeated for several different loop lengths as well as for several different regions of operating frequency. If the difference in length of the two arms of the control loop is known, the change in control frequency can be computed from (9).

If λ_1 and λ_2 in (9) are the free space wavelength, (9) can be written as

$$\frac{2l}{c}\,\Delta f = m, \tag{17}$$

where Δf is the change in control frequency, l is the loop length difference, c is the velocity of light, and m is the phase shift in units of π radians.

If λ_1 and λ_2 are not free space wavelengths, as is actually the case since the microwave energy is propagated in waveguide, then (17) can be written approximately as

$$\frac{2l}{c}\,\Delta f\left\{\frac{\Delta_{av} f_c - \left(\frac{\lambda_g}{\lambda}\right)_{av}}{\left(\frac{\lambda_g}{\lambda}\right)_{av} 2}\right\} = m, \tag{18}$$

where $(\lambda_g/\lambda)_{av}$ is the average value of the ratio of guide wavelength to free space wavelength in the vicinity of f_c, the initial value of the control frequency, and Δ_{av} is the change in $(\lambda_g/\lambda)_{av}$ per megacycle change in the control frequency.

Fig. 5 shows the results obtained in the first series of measurements when the servo loop was balanced manually. Theoretical curves were computed for three different loop lengths using (18). The experimentally determined values are in excellent agreement with the computed values, the largest difference being only on the order of 2 degrees.

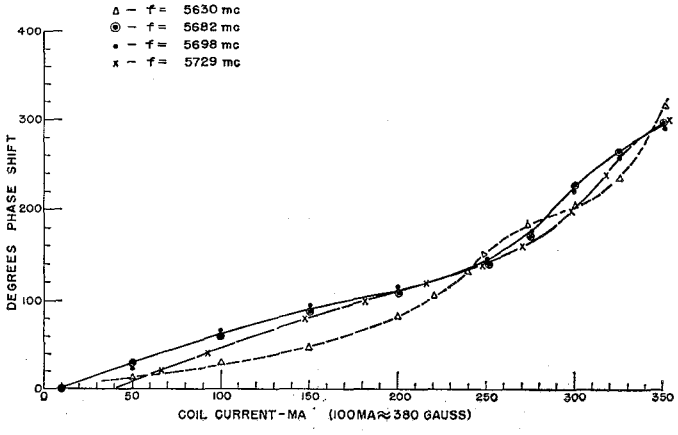

Fig. 7—Ferrite phase shifter characteristics.

Fig. 6 shows the results obtained in the second series of measurements when the servo loop was used as a phase shifter. Eq. (18) was again used to compute the expected phase shift for several values of f_c and for several different loop lengths. In this instance, the measured values of phase shift are not in as close agreement with the predicted values as was the case in the measurements shown in Fig. 5.

The discrepancy between the measured and computed values of phase shift for the data in Fig. 6 is due primarily to the change in the phase shift characteristics of the ferrite phase shifter. Fig. 7 illustrates this. It is apparent that the shape of the phase shift curve changes appreciably with frequency; hence the changes in phase at signal and control frequencies can no longer be expected to track. Even with the very different characteristics shown in Fig. 7, the deviation of the measured phase shift from the computed values is only about 3 per cent of the maximum value of phase shift attained for the higher range in Fig. 6. This could certainly be reduced if the range of control frequencies required for a desired phase shift was reduced by making the loop length difference greater. This would tend to minimize

changes in the shapes of the phase shifter characteristics. A more suitable ferrite or geometry should also reduce this error.

The effect of servo error signal in these measurements is negligible: the gain of the system is sufficient to insure errors of only 2 or 3 degrees.

Conclusion

A control loop has been placed around a ferrite phase shifter to permit precise phase settings. The frequency of a control signal determines these phase settings. The range of control frequencies required can be varied to suit the dispersive characteristics of the ferrite and the stability of the control signal sources. When the duty cycle of the signal whose phase is being shifted is large enough, a heterodyne method can be applied. In this case, the dispersive effects are eliminated as a possible source of error. Preliminary experimental data confirms the expected performance characteristics of the phase control system.

Tables for Cascaded Homogeneous Quarter-Wave Transformers*

LEO YOUNG†

Summary—**Quarter-wave transformers are frequently required in microwave and UHF systems. An exact design procedure is known but involves lengthy calculations. Faced with the design of many such transformers, the calculations were programmed on an IBM 704 digital computer. The speed of computation is such that several hundred designs for 2, 3, and 4 section transformers were systematically computed in a few minutes. The results are reproduced here in tables, which should permit the calculation of most cases of practical interest by interpolation.**

Introduction

MICROWAVE and UHF systems frequently require transformer sections to connect transmission lines of different characteristic impedances with minimum reflection. The multisection quarter-wave transformer serves this purpose well, but it is only comparatively recently that exact design procedures have been published. These are limited to homogeneous transformers, such as coaxial line or E-plane waveguide transformers.

Computation of Impedance Ratios

Design formulas resulting in an equal ripple or Tchebycheff-type response were given by Cohn,[1] Collin,[2]

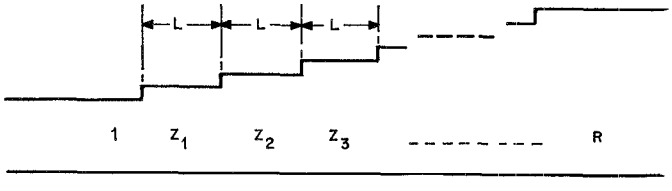

Fig. 1—Quarter-wave stepped transformer.

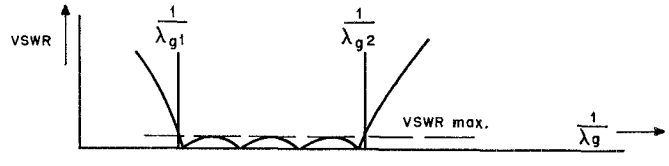

Fig. 2—Typical response curve.

and Riblet,[3] and were experimentally verified. As the computations are somewhat tedious, they were programmed on an IBM Type 704 electronic digital computer for transformers with 2, 3, and 4 sections. For the computation of the characteristic impedance ratios Z_1, Z_2, Z_3, $\cdots$ (Fig. 1), the computer program follows the exact method of Collin and Riblet. The length L of each section (Fig. 1) is nominally a quarter guide wavelength and is defined by

$$L = \frac{\lambda_{g1}\lambda_{g2}}{2(\lambda_{g1} + \lambda_{g2})} \tag{1}$$

where λ_{g1} is the longest and λ_{g2} is the shortest guide wavelength in the pass band (Fig. 2).

* Manuscript received by the PGMTT, August 19, 1958; revised manuscript received, October 22, 1958. This work was part of a project sponsored by the Rome Air Development Center, Rome, N. Y.

† Westinghouse Electric Corp., and The Johns Hopkins University, Baltimore, Md.

[1] S. B. Cohn, "Optimum design of stepped transmission-line transformers," IRE Trans. on Microwave Theory and Techniques, vol. MTT-3, pp. 16–21; April, 1955.

[2] R. E. Collin, "Theory and design of wide-band multisection quarter-wave transformers," Proc. IRE, vol. 43, pp. 179–185, February, 1955.

[3] H. J. Riblet, "General synthesis of quarter-wave impedance transformers," IRE Trans. on Microwave Theory and Techniques, vol. MTT-5, pp. 36–43; January, 1957.